BOREHOLE *IN SITU* INDENTATION TESTS IN FLOATING SEA ICE AT HIGH TEMPERATURES (> 0.97 T_m)

NIRMAL K. SINHA
National Research Council Canada
Building M-17, Montreal Road Complex
Ottawa, Ontario, Canada K1A 0R6

ABSTRACT

Ice is a crystalline material and the temperatures of river, lake or sea ice, floating on its own melt, is close to its melting point. Deformation and failure processes in ice are rate sensitive. They involve high-temperature intergranular cracking and crack-enhanced dislocation creep mechanisms. Moreover, sea ice is like a binary alloy and tends much to loose its inclusions (in this case brine) if sampling is performed when the ambient air temperatures are high. A borehole indentor system was, therefore, developed to determine *in situ* strength and deformation and their rate sensitivity for floating ice covers. This paper describes the methodology used and the results obtained for transversely isotropic columnar-grained, brackish-water ice in a bay in Newfoundland. The tests were carried out at temperatures higher than 0.97 T_m (T_m is the melting point in Kelvin). A Canadian Coast Guard icebreaker was used as the floating laboratory.

KEYWORDS

In situ, borehole indentation, creep, strength, floating sea ice, rate sensitivity, ice breaker

INTRODUCTION

In addition to the multitude of structural features, natural ice shows a great deal of trapped impurities depending upon the purity of the water or the melt from which the ice grew. Sea ice is like a binary alloy and contains a significant amount of brine, in addition to air, in the form of pockets trapped between the grains and the subgrains. Desalination is possible if blocks of ice are to be recovered and shipped for conducting laboratory tests. This is a chronic problem in the sampling and testing of sea ice, especially when the ambient air temperatures are higher than about - 15 °C or 0.95 T_m.

Devices have been developed for *in situ* tests, namely the borehole pressuremeter (Murat et.al., 1986; Shields et. al., 1989), the borehole jack (Iyer and Masterson, 1991; Sinha, et. al. 1986; Sinha, 1987) and flatjack (Comfort and Ritch, 1990). After evaluating the existing systems (Sinha, 1987), a new borehole indentor system was developed by the author at the National Research Council Canada (NRCC) to conduct *in situ* strength tests in ice.

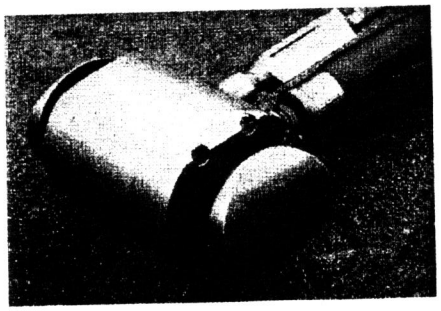

Fig. 1.

Top) The complete NRCC borehole indentor test system on the ice in the Bay of Exploits near Botwood, Newfoundland in front of the icebreaker CCGS "Sir John Franklin".

Left) The borehole indentor with curved stainless steel polished plates.

The NRCC borehole indentor system was used for evaluating the decay processes in a fresh-water lake ice cover (Sinha, 1990) and for evaluating the rate sensitivity of 'Ice Island' multi-year sea ice (Sinha, 1991) and shelf ice. It proved ideal for determining *in situ* mechanical behaviour of land-fast brackish-water sea ice in the 'Bay of Exploits', near Botwood, Newfoundland (49.2N, 55.3W), during the multidisciplinary, international "Labrador Ice Margin Experiment 1989" (LIMEX-89) program. The Canadian Coast Guard Ship (CCGS) "Sir John Franklin" was used as the working platform (Fig.1).

NRCC BOREHOLE INDENTOR SYSTEM

The NRCC borehole indentor system consists of three major components: 1) a fibre-glass ice core auger, 2) a stainless steel (100%) indentor and 3) a portable power supply for the hydraulic system and the data loggers. The motor-driven core auger makes 150 mm diameter, smooth-walled, vertical boreholes in the ice. It also provides 100 mm diameter ice cores for examination and characterization of the ice to be tested. The indentor operates in the borehole and can be lowered down to a depth of 5 m. Load is applied hydraulically to push two polished plates on opposite ends

of the jack against the sides of the borehole. The loading rates can be varied by controlling the hydraulic fluid flow rate. The 90 mm diameter plates are curved in one plane to match the curvature of the wall (Fig.1, left). A transducer in the hydraulic system is calibrated to give the average applied pressure on the plates, and two LVDT type displacement gauges provide data on the relative and total diametral displacement of the plates into the ice. The system is powered by a 110 volt electric generator. During a test, the output from the pressure transducer and the two displacements gauges is recorded as a function of time, using a strip chart recorder as well as a digital data logger. There is also a provision for manually recording the plate pressure registered on a dial gauge attached to the supply line (electronic systems often do not work at extremely low temperatures).

The entire borehole indentor system can be transported by a helicopter or can be mounted on a Komotik (sledge) for moving it from a base camp to a test site using a snowmobile.

In Situ FIELD TESTS IN BOTWOOD BAY

The present test series was carried out during the evening of 9 March and during the early morning of 10 March. During this time, the icebreaker, CCGS "Sir John Franklin" was stopped at position 49.2N, 55.3W in the landfast ice in Bay of Exploits near Botwood, Newfoundland, Canada. Experiments were carried out in a flat area of 125 m x 150 m where there was no ridging or rafting in the immediate area. Here, the surface of the ice was completely covered with a thin layer of snow of average thickness 0.06 m ± 0.02 m; the average ice thickness was 0.63 m ± 0.03 m (14 measurements). The air temperatures during the test periods varied between -7 °C and -10 °C. The snow/ice interface temperature was measured at several locations. The average value was found to be -7 °C ± -1.3 °C (Nazarenko and Lapp, 1989).

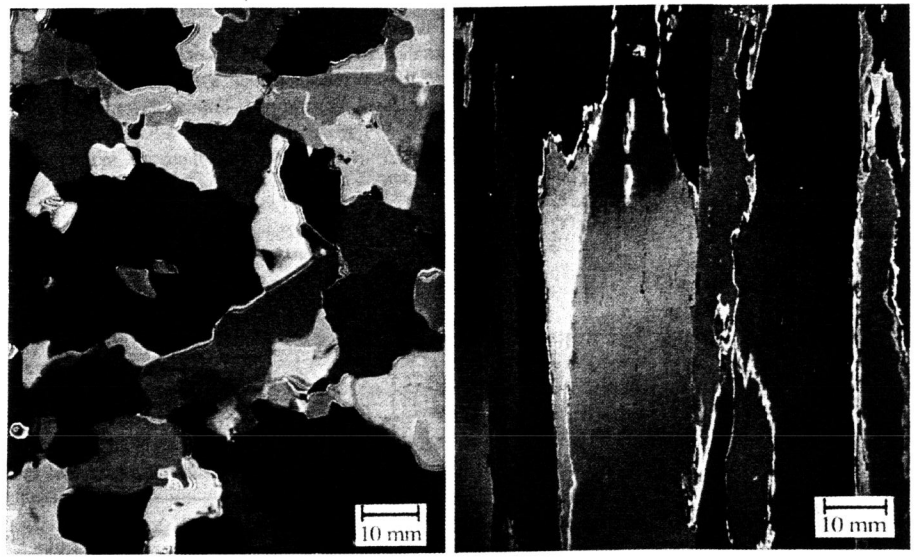

Fig. 2. Horizontal (left) and Vertical (right) thin sections of transversely isotropic clear, columnar-grained ice at Botwood Bay, photographed under crossed polarized light.

After drilling a hole each core was examined to characterize the ice. It was noticed that the ice consisted of two main layers. About 0.20 m at the top was dense, isotropic equiaxed snow ice. The rest of the ice was clear columnar-grained (Fig. 2). Indentation tests were conducted by lowering the indentor to a depth of 0.35m to be well within the columnar-grained ice zone. At this depth, the ice temperature was about - 3.5 °C, equivalent to a homologous temperature of 0.98 T_m. The distance between the holes was kept to about 2 m or more in order to avoid any damaged zone created in the ice by the tests. To avoid any change in the thermal regime of the ice, each hole was drilled immediately before the test. From the beginning of drilling to the start of a test, the total time was reduced to a few minutes at Botwood. Both displacement history and the pressure history were recorded separately on strip-chart recorder as well as by a digital recorder. For evaluating the rate sensitivity of the ice response, tests were performed at several rates of loading.

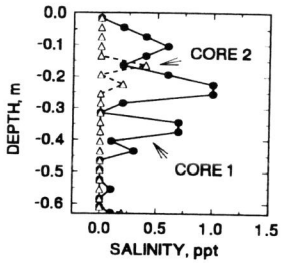

Fig. 3. Vertical salinity profile of ice tested.

In all, 26 tests were carried out at the Botwood site. Three of the 26 full-thickness ice cores recovered, were taken to the icebreaker immediately after sampling and were stored in a deep freezer kept at - 20 °C. One of the cores was examined for microstructural analysis and other two were sectioned for determining vertical salinity profiles in the ice. A sample of water, below the ice cover, was also taken for measuring the salinity of the water in the bay.

ICE CHARACTERISTICS

Figure 2 shows the grain structure of the columnar-grained zone of the ice cover. Note the sutured characteristics of the grain boundaries. The salinity of the ice was low (Fig. 3). The average value was about 0.3 parts per thousand (ppt). This low level of trapped impurities substantiates observations of the solute concentration in the water below the ice cover of only 8.8 ppt compared to the open sea water salinity of about 34 ppt. The solute concentration in annual sea ice, in the polar regions of both the Arctic and the Antarctic, is about 5 ppt. The water in the Botwood Bay, and hence the ice tested was brackish.

RESULTS AND ANALYSIS

Stress (average plate pressure) - indentation (half of the total diametral displacement) curves for a rapid test and a slow test are shown in Fig. 4. In both cases, the stress increases with the increase in indentation and reaches a peak value after which it decreases with further indentation. The maximum value or the failure stress, σ_f, the slope of the stress-indentation curves before failures and the rapidity of the pressure drop during the post-failure period - all depend upon the rate of loading.

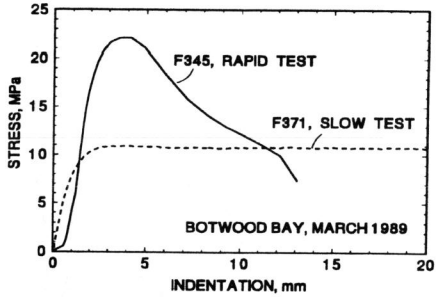

Fig. 4. Stress-indentation curves for two tests

Stress-indentation curves, like usual stress-strain diagrams, do not show the time aspects of the tests under examination. At elevated temperatures, where the mechanical response of materials is governed by dislocation-creep and rate sensitive kinetics of microcracking, the histories of stress and strain (indentation in the present case), provide much more valuable information (Sinha, 1982).

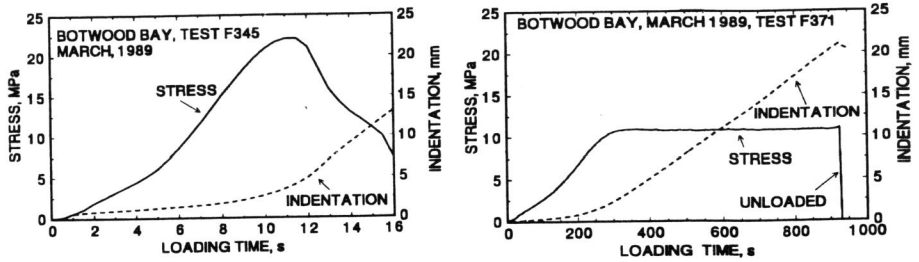

(a) (b)

Fig. 5. Stress and indentation histories for the rapid (a) and the slow (b) tests for the results in Fig. 4.

As can be seen in Fig. 5a and 5b, the indentation rate, irrespective of the rapidity of the tests, was not constant during the loading period until after reaching the peak load. This is because the rate of indentation was not controlled by any closed-loop control - a difficult tasks to incorporate in field equipments subjected to extreme environmental conditions.

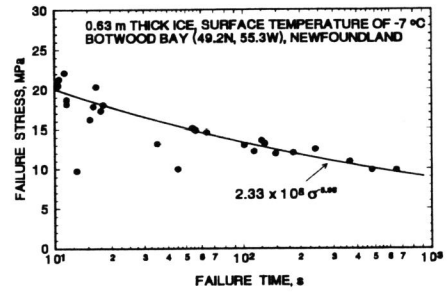

Fig. 6. Failure time versus failure stress.

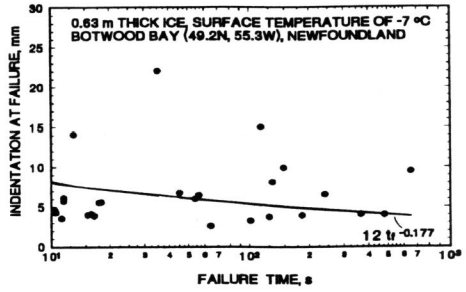

Fig.7. Failure time versus failure indentation.

Due to the nonuniform indentation rate during the pre-failure period, the average indentation rate to failure, defined as $\dot{d}_{af} = d_f / t_f$, or the average stress rate to failure, given by $\dot{\sigma}_{af} = \sigma_f / t_f$, are good measures of the loading conditions (Sinha, 1990, 1991). These quantities can be obtained from the information on the dependence of failure stress on failure time (Fig. 6) and the dependence of the depth of indentation at peak load on failure time (Fig. 7). For example, the indentation at failure, d_f, corresponding to the peak load of 22.1 MPa at the failure time, t_f, of 11.3 seconds, in the case of the rapid test in Fig. 5a, is 3.57 mm, giving an average stress rate to failure of 2.01 MPa.s^{-1} and an average indentation rate to failure of 0.32 mm.s^{-1}.

The effect of loading rate or indentation rate on strength and deformation are evident in Fig. 8 and Fig. 9. The loading rate seems to influence the failure stress more significantly than the displacement at failure. Similar rate effects were also seen in first-year sea ice in the high Arctic (Sinha 1987).

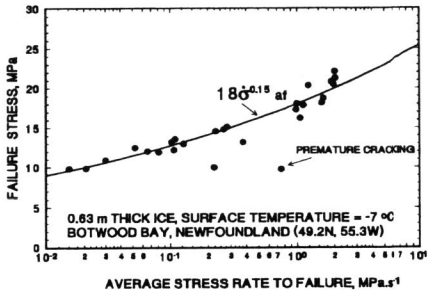

Fig. 8. Failure stress versus stress rate.

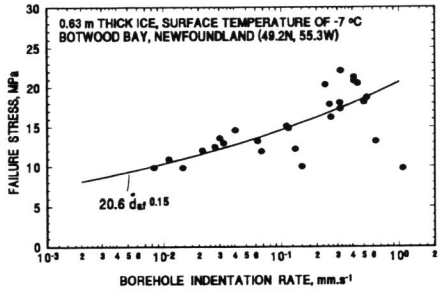

Fig. 9. Indentation rate dependence of stress.

Since the load and the time can be measured more accurately than the depth of penetration, emphasis will be given first to the interrelationship between the failure stress and failure time (Fig. 6). This dependency may be expressed by:

$$t_f / t_o = C (\sigma_f / \sigma_o)^{-\theta} \qquad (1)$$

where t_o is the unit time (1 second) and σ_o is the unit stress (1 MPa). Regression analysis provided the value of $C = 2.33 \times 10^8$ and $\theta = 5.66$, giving $t_f = 2.33 \times 10^8 \, \sigma_f^{-5.66}$, as can be seen by the solid line in Fig. 6. There is a remarkable similarity between this relationship and the dependence of creep rupture time on stress for metals and alloys at high temperatures (Garofalo, 1965) and pure ice (Sinha, 1982).

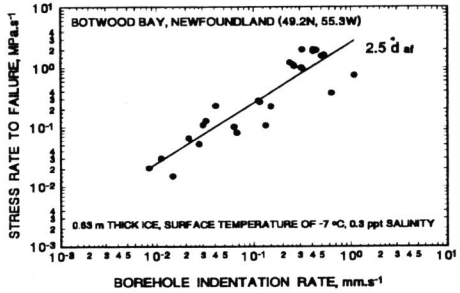

Fig. 10. Stress rate versus indentation rate.

By rearranging Equation (1), and remembering $\dot{\sigma}_{af} = \sigma_f / t_f$, the dependence of failure stress on average stress rate can be obtained,

$$\sigma_f / \sigma_o = C^{1/1+\theta} (\dot{\sigma}_{af} / \dot{\sigma}_o)^{1/1+\theta} \qquad (2)$$

where $\dot{\sigma}_o$ is the unit stress rate (1 MPa. s^{-1}). On substitution of the values of C and θ, Equation (2) reduces to $\sigma_f = 18 \, \dot{\sigma}_{af}^{0.15}$ as shown in Fig. 8.

Figure 10 shows that there is a linear relationship between the average stress rate to failure and the corresponding average indentation rate, defined as $\dot{d}_{af} = d_f / t_f$, so that,

$$\dot{\sigma}_{af} / \dot{\sigma}_o = E (\dot{d}_{af} / \dot{d}_o) \qquad (3a)$$

or

$$\sigma_f / \sigma_o = E (d_f / d_o) \qquad (3b)$$

where $\dot{d}_o$ is the unit indentation rate (1 $mm.s^{-1}$ in the present case) and E may be identified as the failure stiffness of ice. The solid line in Fig. 10 gives E = 2.5 MPa/mm. Equations (2) and (3a) can be combined to obtain the dependence of failure stress on average indentation rate to failure,

$$\sigma_f/\sigma_o = (CE)^{1/1+\theta} (\dot{d}_{af} / \dot{d}_o)^{1/1+\theta} \qquad (4)$$

or $\sigma_f = 20.6 \, \dot{d}_{af}^{0.15}$, on substitition of the values of C, E and θ, (Fig. 9). This is analogous to the well known Norton's power law describing the stress dependence of minimum creep rate in constant stress creep tests (see, for example Odqvist, 1974).

Equations (1) and (3a) can be combined to show that

$$t_f / t_o = (EC^{-1/\theta})^{-\theta/(1+\theta)} (\dot{d}_{af} / \dot{d}_o)^{-\theta/(1+\theta)} \qquad (5)$$

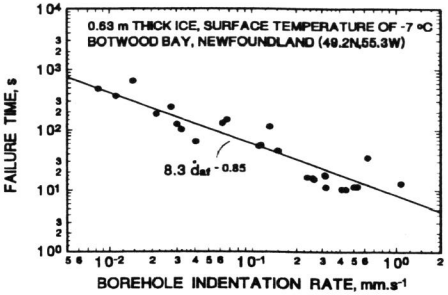

Fig. 11. Failure time versus indentation rate.

which, on substitution of the values of C, E, and θ, reduces to $t_f = 8.28 \, \dot{d}_{af}^{-0.85}$ as can be seen in Fig. 11. This approximate inverse proportionality between failure time and indentation rate is analogous to the empirical Monkman-Grant relation between rupture time and minimum creep rate.

Equations (1) and (3b) gives $d_f / d_o = (C^{1/\theta} / E) (t_f / t_o)^{-1/\theta}$ (6)

which, on substitution of the values of C, E, and θ, simplifies to $d_f = 12 \, t_f^{-0.177}$. Failure indentation does not, therefore, vary much with failure time. Analogous behaviour has been observed in metals and alloys during tensile creep rupture or fracture experiments. Creep ductility has been found to be relatively insensitive to a wide variation of stress and creep life. When nucleation and growth of cavities are responsible for creep failure, the strain at fracture has been reported to be almost independent of stress and hence strain rate in metals and alloys (Garofalo, 1965; Greenwood, 1973).

CONCLUSIONS

The NRCC borehole indentation system was found to be mobile and rugged for quick deployment on an ice cover from an icebreaker. It was found suitable for determining *in situ* confined strength and deformation of floating sea ice at temperatures close to its melting point. Indentation strength was found to be rate sensitive and analysis must include load and displacement history. Ideally, the rate of indentation should be controlled by a closed-loop system - a difficult task to incorporate in field equipment. Since the indentation rate was not controlled in the present tests, the average displacement rate to the maximum stress (plate pressure) and/or the average stress rate to failure were found appropriate for the analyses. The results bear one to one correspondence to the creep-rupture/fracture response commonly seen in polycrystalline materials in general. The average indentation rate was noted to be analogous to the minimum creep rate in constant-stress creep tests or the strain rate in constant strain-rate strength tests. The present test series confirmed the fact that ice mechanics is part of a broad subject: high temperature creep, structural damage and failure of polycrystalline materials. The test program points out that natural ice is an ideal material for studying advanced high-temperature engineering materials at extremely high homologous temperatures and that the rate-dependent indentation tests could be extended to other materials.

ACKNOWLEDGEMENTS

The author acknowledges the assistance provided in the field by R. Jerome, C. A. Bjerkelund, D. Lapp and D. Nazarenko. He is indebted to Canada Centre for Remote Sensing for providing the travel funds to Newfoundland, and the Canadian Coast Guard for providing all the logistics at sea.

REFERENCES

Comfort, G., and Ritch, R. (1990). Field measurement of pack ice stresses. In: Proc. 9th. Int. Conf. Offshore Mechanics and Arctic Engineering (OMAE), Vol. 4, pp. 177-181, Am. Soc. Mech. Eng.(ASME), New York.

Garofalo, E. (1965). Fundamentals of creep and creep rupture in metals. Chapters 6 and 7, MacMillan, New York.

Greenwood, G.W. (1973). In: The microstructure and design of alloys, pp.91-105. The Institute of Metals and The Iron and Steel Institute, London

Iyer, S.H., and Masterson, D.M. (1991). Field strength values of multi-year ice off Herschel island. In: Proc. 10th. Int. Conf. Offshore Mechanics and Arctic Engineering (OMAE), Vol. 4, pp. 63-70, Am. Soc. Mech. Eng.(ASME), New York.

Murat, J.R., Huneault, P., and Ladanyi, B. (1986). Effects of stress redistribution on creep parameters determined by a borehole dilatometer test. In: Proc. 5th. Int. Conf. Offshore Mechanics and Arctic Engineering (OMAE), Vol.4, pp. 58-64, Am. Soc. Mech. Eng. (ASME), New York.

Nazarenko, D. and Lapp, D. (1989). Ice Characterization Studies from the CCGS Sir John Franklin. In: LIMEX 1989 Data Report, Section 7.7, 47 pages. Canada Centre for Remote Sensing, Energy, Mines and Resources, Ottawa, Canada.

Odqvist, F.K.G. (1974). Mathematical theory of creep and creep rupture. Second Edition, The Clarendon Press, Oxford.

Shields, D.H., Domaschuk, L., Funegard, E., Kjartanson, B.H., and Azizi, F. (1989). Comparing the creep behaviour of spray ice and polycrystalline freshwater ice. In: Proc. 8th. Int. Conf. Offshore Mechanics and Arctic Engineering (OMAE), Vol.4, pp. 235-245. Am. Soc. Mech. Eng. (ASME), New York.

Sinha, N.K. (1982). Constant strain- and constant stress-rate compressive strength of columnar-grained ice. J. Mat. Sci., **17,** 785-802

Sinha N.K., Strandberg, A. and Vij, K.K. (1986). In situ assessment of drilling platform sea ice strength using a borehole jack. In: Proc. In-situ Testing and Field Behaviour, 39th Canadian Geotechnical Conference, pp.153-157, Canadian Geotechnical Society, Ottawa, Canada.

Sinha, N.K. (1987). The borehole jack - is it a useful Arctic tool? J. OMAE, Transactions of the Am. Soc. Mech. Eng. (ASME), **109**,391-397.

Sinha, N.K. (1990). Ice cover strength decay using borehole indentor. In: Proc. IAHR Symposium on Ice, Vol.2, pp 735-744, Helsinki University of Technology, Espoo, Finland.

Sinha, N.K. (1991). In situ multi-year sea ice strength using NRCC borehole indentor. In: Proc. 10th. Int. Conf. Offshore Mechanics and Arctic Engineering (OMAE/ASME), Stavanger, Norway, June 23-29, 1991, Vol. 4, pp. 229-236, Am. Soc. Mech. Eng. (ASME), New York.